

Visual localization with Vestibular input

Wouter Mattheussens

S4198905

Prof. Dr. J.A. Van Opstal, Dr. A.D. Barsingerhorn, J.J. Heckman (MSc)

25-08-2020



Table of Content

Abstract	3
1. Introduction.....	4
2. Methods	7
2.1 Vestibular setup.....	7
2.2 Subjects	7
2.3 Measurements	8
2.4 Localization experiment with vestibular input.....	8
2.5 Data analysis.....	9
2.7 Modelling.....	10
2.8 Statistics.....	12
3. Results	13
3.1 Gaze saccade consists of an Eye and Head component.....	13
3.2 Target vs. Response in chair coordinates	14
3.3 Target versus Response with different models.....	16
3.4 Stimulus duration versus Reaction times	23
4. Discussion.....	25
References.....	28

Abstract

To localize objects in space, the visuomotor system must incorporate visual input from the retina with extraretinal input, to be able to distinguish target motion from self-motion. By doing this, the visuomotor system can account for intervening head and eye movements that are being made between the presentation of a visual stimulus, and the initiation of a goal directed saccade towards the location of the visual stimulus. This process is called spatial updating. However, the question arises how much information about target motion and self-motion is needed for spatial updating. To investigate this, we asked our subjects (n=5) to localize visual flashes, while they were being passively rotated around the vertical axis in a sinusoidal pattern. Subsequently, we examined eight models that accounted for passive head-in-chair movements, active head movements and/or eye-in-head movements between stimulus onset and saccade onset. After that, we compared the localization results of our subjects with the predicted response based on each of the models. Furthermore, we investigated whether the saccade latencies depended on stimulus duration. Our results show that during both the head free- and head fixed condition, the localization behaviour of our subject could best be explained if the visuomotor system compensated for intervening active head movements and eye-in-head movements, but not for passive head movements. Additionally, we found that the reaction times were significantly shorter for the 100ms stimulus duration, compared to the shorter stimulus durations. Thus, the results of this internship report suggest that the visuomotor system of our subjects used spatial updating to localize the targets for both the head free and head fixed condition for all stimulus durations and that the reaction times were shorter for the 100ms stimulus duration.

1. Introduction

To perceive the world around us, humans incorporate sensory stimuli of various natures, such as tactile-, olfactory-, auditory-, visual- and vestibular stimuli. By incorporating these stimuli in the brain and processing them, we are able to produce responses to the stimuli we deem interesting. These responses we call behaviour. However, the underlying neural mechanisms between perceiving a stimulus and the subsequent response are often complex and not fully understood.

In order to adequately locate objects in space, the visuomotor system incorporates input from the target location and redirects the eye and head as output. The cumulative relocation of the eye and head is called a gaze shift (gaze \equiv eye-in-space + eye-in-head + head-in-space) and the fast, voluntary orienting response of the eye is known as a saccade^{1, 2}.

Furthermore, to keep track of objects in the world around us, it is key that we are able to identify whether they are stationary or moving through space. Especially in relation to our own movement. As such, the brain must take two factors into account to perform an accurate gaze shift towards a presented object. First, the brain must identify where in space the object is presented in relation to the location of retina in space (i.e. the retinal error). Second, the brain must incorporate self-motion in order to compensate for any movement that was made after the presentation of the object. When these factors are combined, the subject should have an accurate representation of the target location to be able to make a saccade to localize the target in space. The process of combining the retinal error and intervening movements is called spatial updating³.

To incorporate spatial updating, the visuomotor system should incorporate information such as neck muscle proprioception⁴, corollary discharges and efference copies⁵, and vestibular signals⁶ to constantly update the internal representation of the target's location⁷. It has also been suggested that eye muscle proprioception might contribute to the detection of self-motion. However, whether this is true or that self-motion is established based on an efference copy of the motor command from the eye movement, remains a topic of debate⁸. Nevertheless, when the system is deprived of most extraretinal information, such is the case as when the head is fixed, we assume that the visuomotor system can only rely on the image that is projected on the retina and the input from the vestibular canals to discriminate between target and self-motion.

The perception of the image that is projected on the retina is dependent on three factors: the duration and the intensity of the stimulus, and the location on the retina. As a source emits light (e.g. a visual stimulus), photons reach the photoreceptors on the retina, which cause a hyperpolarization of the photoreceptors and a subsequent depolarization of the underlying ON-bipolar cells. In darkness, the photoreceptors are depolarized and excitatory neurotransmitters (glutamate) depolarize the OFF-bipolar cells⁹. Finally, the bipolar cells connect to the amacrine- and direction selective ganglion cells, in which it is believed that motion detection is established. Although the exact computational mechanisms of motion detection are not fully understood, it is hypothesized that these cells utilize a delay-and-compare mechanism to generate a direction selective output¹⁰. One such delay-and-compare model is the Hassenstein-Reichardt-model¹¹. In this model, the sequence of firing bipolar cells (A, B) is compared in the direction selective cells (C) in space and time. By delaying the input from cell A and measuring the output in (C), one can establish whether cell A fired before cell B. As such, motion detection can be established.

Thus, it might be that early direction selection is already located on the retina. From there, the signals are propagated to other brain areas, in which the actual perception of motion is established,

such as brain area V5¹². Nonetheless, the information that is gained by these processes determines whether the target has moved in space over time when the object moves, and the observer is stationary.

However, in natural environments, the observer itself is rarely stationary. In other words, the visuomotor system also has to compensate for self-motion. For the perception of self-motion, various brain areas are be involved¹³. However, the vestibular primary afferents mainly project to the vestibular nuclei, thalamus and posterior cerebellum and come from the vestibular organ¹⁴. The vestibular organ is located in the inner ear and consists of three semi-circular canals (superior, posterior, and horizontal) and two otolithic organ (the utricle and saccule). The semi-circular canals respond to rotational acceleration, whereas the utricle and saccule respond to linear acceleration and gravitational acceleration, respectively⁹. During horizontal rotation, potassium rich endolymph in the horizontal semi-circular canal causes the stereocilia to deflect towards or away from the kinocilia in the ampulla. This results in either a depolarization or hyperpolarization of the underlying hair cells, respectively¹⁵. The subsequent release of neurotransmitters cause the signal to propagate towards the vestibular nuclei¹⁶. For further processing of the perception of self-motion, the vestibular nuclei project towards a network of different brain areas, including the cerebellum, thalamus and parietoinsular vestibular cortex (PIVC)¹³.

During self-motion it is important to keep a stationary image, as otherwise motion blur may occur². To maintain this stable image despite self-motion, the vestibular nucleus from one side innervates the contralateral abducens nucleus, which in turn causes a contraction of the medial and contralateral eye muscle. Importantly, the semi-circular canal on the other side of the head hyperpolarizes its respective vestibular nucleus, which in turn inhibits its own contralateral nucleus that causes the relaxation of the medial and contralateral eye muscles. This 'Push-and-Pull' system between the two semi-circular canals results in a correcting eye movement towards the fixation point, which we call the vestibulo-ocular reflex¹⁷. When a subject is passively rotated in a sinusoidal pattern, there is a constant VOR towards the fixation point. As a result, the eyes move constantly in the head in the opposite direction of the sinusoidal movement. This eye movement is called the vestibular-ocular nystagmus and it consists of a slow-phase and a quick-phase. The slow phase is categorized by the compensatory movements of the eyes contradictory to the head. Meanwhile, the quick-phase functions as a reset for the slow-phase by recentring the eyes to the middle of the head¹⁸. The direction of the quick-phase is opposite of the direction of the rotation. During prolonged rotational self-motion (more than 7s) the VOR disappears. This process can be modelled as a leaky integrator and it is thought this prevents unwanted eye movements during constant motion^{19, 20}. To quantify the VOR and vestibulo-ocular nystagmus, the 'gain' is calculated. The gain represents the change in eye movement in relation to the change in head movement. During a typical VOR as a result of head movement, the gain of a VOR would be 1. However, as the vestibulo-ocular nystagmus is dependent on the frequency and velocity of the rotation, the gain is often lower than 1²¹. Finally, as the size of the VOR is increased in relation to higher frequency horizontal head movement, the vestibular organ acts as a high-pass filter²².

Thus, when the vestibular system provides information regarding self-motion and the retinal signal provides information about the target motion, the visuomotor system should be able to produce the correct gaze shift to localize a target. However, how do these factors relate to each other and how much retinal information is needed to correctly localize a target in space during self-motion? In an attempt to answer these questions, a study by Van Barneveld et al.²³ asked subjects to localize targets in space that were presented as visual flashes with various stimulus durations, while being passively rotated horizontally in a sinusoidal pattern. To determine whether or not the subjects used

spatial updating to localize the targets, they proposed four models that each compensated for either the head movement in space, or eye-in-head movement (or both or none). They found that during long flash stimulus duration (100ms), spatial updating was present and intervening eye and head movements were fully accounted for. However, during short stimulus durations (0.5ms), there was no compensation for these factors and stimuli were localized from a retinocentric perspective.

To elaborate on these findings, the aim of this report is to further investigate the dynamics of stimulus duration and spatial updating. As such, we will perform visual localization experiments on both head fixed and head free subjects, that are being rotated sinusoidally in a chair along the vertical axis, while presenting flash stimuli with different stimulus durations. Importantly, the stimuli that we present are fixated to the chair. As such, they are presented to the subject in coordinates relative to the head, in contrast to world coordinates.

To investigate which factors are incorporated in the production of a gaze shift under experimental conditions, we can analyse the gaze-shift according to the models proposed by Van Barneveld et al.²³ and Vliegen et al.²⁴. However, Van Barneveld defined head movement as a shift of 'head-in-space', which represented the passive head movement of the head as a result of the horizontal movement of the rotation. However, as our subjects will not be head fixed in one condition, we expand upon the models of Van Barneveld by further separating the movement of the head into a passive component (chair in space) and an active component (head in chair). As such, we propose eight different models, that aim to explain the localization errors that have been made, by compensating for either intervening passive head movements, active head movements or eye-in-head movements. We will elaborate further on the mechanisms of these models in the methods section. However, we expect that the subjects will opt for a strategy that compensates for the intervening active head movement and eye-in-head movement, but not for the passive head movement. As the targets are fixated to the chair, the relative difference in motion between the target and the subject is 0. As such, there would be no need to compensate for the movement of the chair.

Thus far, we aim to explain the localization behaviour of our subjects with the eight different models. However, these models are based on the accuracy of the response as a function of the strength (duration) of the stimulus, which is also known as a psychometric function²⁵. In addition to psychometric performance, one could look at the chronometric performance, which measures the reaction time as a function of the stimulus strength. To do this, we aim to investigate the influence of stimulus duration on the latency between the stimulus onset and the start of the saccade. It is known that the ambiguity of a stimulus affects the reaction time of the subject to that given stimulus²⁶. For example, when subjects were asked to press a button upon a stimulus presentation, the mean reaction times decreased with an increasing luminance of the stimulus. As shorter stimulus durations are generally harder to detect than longer stimulus duration, we expect that shorter stimulus have a longer reaction time.

In summary, during our experiments, we expect that the spatial updating in our subjects is determined by the active head movements and eye movements, but not the passive movement of the head in the chair. Furthermore, we aim to investigate the influence of stimulus durations on the latency between the stimulus onset and start of the saccade. Here, we expect that the shorter the stimulus duration, the longer the reaction time.

2. Methods

2.1 Vestibular setup

Experiments were performed in a 2-axis, servo controlled vestibular stimulator (or vestibular chair, VC), that allows for rotations along the x-, y- and z-axis. The room in which the experiment was performed was approximately 19m² and shielded with black acoustic foam (Uxem, Lelystad) that absorbs all frequencies below 500Hz, leaving a background noise level of 45.3dBA. Visual stimuli were presented by 38 speaker-LED-combinations (SLCs). The speakers (7.8x7.8x7.8cm, Cambridge Audio MINX MIN12, Cambridge) were equipped with red/green LEDs (BIVAR 5BC-3-CA-F; peak wavelengths: 625nm and 568nm) in the centre. As depicted in Figure 2, each SLC was spaced 10° from one another. The range of the setup was $\alpha = [-30\ 30]$ and $\epsilon = [-30\ 30]$ and the setup was placed 1m from the subjects' head. To be able to distinguish between a quick phase of the vestibulo-ocular reflex during rotation and a response saccade, we excluded the SLCs at $\epsilon=0$. As such, each goal directed saccade had an elevation component which facilitated the saccade detection.

2.2 Subjects

In total, six subjects (5 male, 1 female; mean age = 26.8±1.4) participated in the experiments. Except for subject S001, all subjects wore glasses, which they removed for the experiments. However, all the subjects were able to see the stimuli that were presented to them for all stimulus durations.

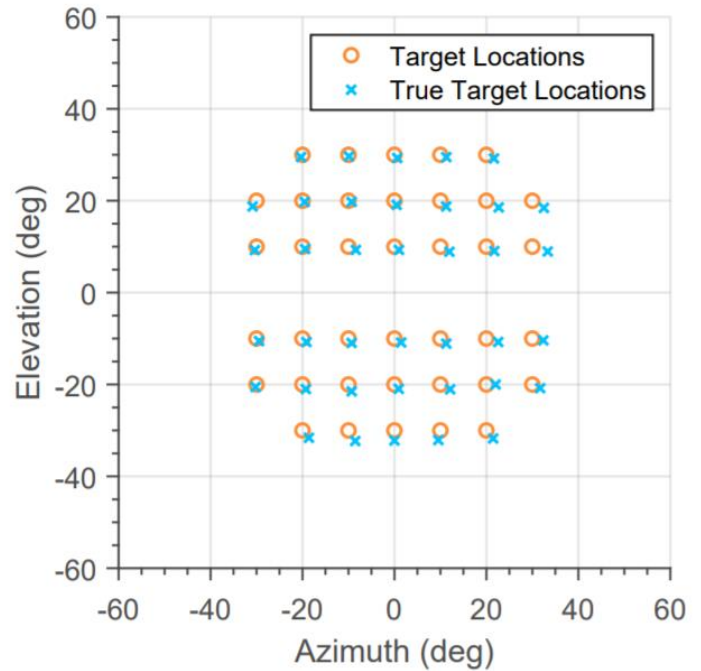


Figure 1: Overview of 38 stimulus locations. X-axis displays the azimuth in degrees, while the y-axis displays the elevation in degrees. The orange targets display the theoretical target locations. The blue target locations display the actual measured target locations in chair coordinates.

2.3 Measurements

To measure the eye- and head movements of the subject, the Pupil Labs System and the Optitrack Trio System were used, respectively. The Pupil Labs system consisted of a separate PC, Pupil Capture software (Pupil-Labs) and a spectacle frame with an infrared (IR) world camera (Global Shutter: 1280x720 @60fps) and an IR eye camera (Global Shutter 200x200 @60fps, 400x400 @120fps). The world camera was used for calibration and the eye camera was used to record the eye data. During the calibration of the eye tracker, subjects had to fixate their eyes on a marker provided by the experimenter. Subsequently, they had to move their head in all directions, to determine the degrees of offset. The calibration was deemed as acceptable when the mean absolute offset was lower than $2.5^\circ \pm 0.2\text{std}$.

The Optitrack Trio System was used to measure the head movement during the experiment and consisted of a headband with IR rigid-body markers (Optitrack), the Optitrack PC and Motive software (Optitrack).

The experiments were initiated using vPRIME, created by J.J. Heckman. This custom-built MATLAB (Mathworks) software toolbox with graphical user interface allowed for the loading of EXP-files, which contained the necessary information about the number of blocks, trials, and stimuli. This information was subsequently sent to the Tucker Davis Technologies (TDT) system, which was responsible for the execution of the experiment by presenting the stimuli to the SLCs and vestibular chair motors. After the stimuli had been presented and the data had been recorded, the data was stored in MATLAB.

Simultaneously, the Lab Streaming Layer (LSL) recorded separate timestamps, which were also stored in MATLAB.

2.4 Localization experiment with vestibular input

Before the experiments were conducted, all subjects were instructed about the experiments. Each experiment consisted a head-free and head-fixed condition and each condition consisted of 28 blocks of 41 trials of approximately 3s each. Measurements were done over two days with 28 blocks per day. During the first day, the blocks 1 to 14 were defined as the 'Head-fixed' condition. Subjects were asked to make an orienting response towards the vestibular stimuli using their eyes, while keeping their head still. During block 15 to 28, the subjects were asked to also include head movements during their response; the 'Head-free' condition. The second day, this pattern was reversed. As such, 28 blocks per condition were measured for these subjects. For subject S001, the 'Head-free' condition consisted of 24 blocks of 48 trials of the first day and the 'Head-fixed' condition consisted of 28 blocks of 41 trials on the second day. Furthermore, the subjects were asked to fixate on a fixation light that was presented at the central SLC ($\alpha = 0$, $\epsilon = 0$) for a duration of 5 seconds at the start of the experiment before the trials started. Finally, the subjects were instructed to return their gaze towards the central SLC, after they had fixated on the target location for a short moment.

After the subjects were instructed and calibrated, the experiments were performed in complete darkness. During the experiments, the subjects were rotated along the vertical axis at $70^\circ/\text{s}$ with a frequency of $1/2\pi$ Hz, visual stimuli were presented as a flash with a duration of 0.5, 1, 2, 4 or 100ms at the target location. Both the locations and stimulus durations were randomly generated for all blocks combined, and subsequently divided over 28 blocks. In total, each stimulus duration was presented approximately 230 times over the 38 stimulus locations. Moreover, to prevent that the subjects learned when the stimulus onset would be presented, the time between two stimuli was 3s with a random interval of $\pm 500\text{ms}$. To prevent fatigue and the loss of concentration, a break was held every seven blocks. However, if necessary, participants were able to take more breaks.

2.5 Data analysis

After the data had been recorded, data analysis was performed off-line using MATLAB. First, the eye- and head data were imported, together with their respective LSL-timestamps. Subsequently, we synchronized the data based on the LSL-timestamps. To construct the gaze, we first interpolated the eye data to the timestamps of the head data, so that they were equal in length and could be combined. After that, we converted the eye- and head data to rotation matrices. We converted the head data from quaternions to a rotation matrix and we converted the eye data we to a unit vector and via quaternions to a rotation matrix. To determine where the centre ([0,0]) of the eye- and head data were, we assumed that the subjects fixated on the fixation LED at the start of each block, which we took as a reference point. After both the eye- and head data were converted to rotations matrices, we combined them to create the rotation matrix for the gaze, according to the method proposed by Ronsse et al.²⁷ From the rotation matrix of the gaze, we formed the azimuth and elevation vectors, which we also recentred for gaze = 0. Moreover, we interpolated the gaze vectors to the timestamps of the head data. Subsequently, we extracted the relevant data by epoching the gaze data from the stimulus onset to the end of the trial. After that, we stored the epoched azimuth- and elevation data of the gaze as .hv files. The .hv files were further analysed in SacDet (Marc van Wanrooij, 2007). SacDet is custom made Matlab software which is used to detect saccades based on velocity ($>30^\circ/s$), amplitude ($>4^\circ$), duration ($>20ms$) and reaction time (between 80ms and 800ms). Each identified saccade was manually verified by the experimenter to ensure the validity. As quick phases of the vestibulo ocular nystagmus can be detected as saccades based on their velocity and amplitude, the distinction between a quick phase and a saccade was made based on the elevation component of the eye movement because only the saccades were expected to have an elevation component. Furthermore, when the saccade also included a prolonged fixation on the target, the length of the saccade could be adjusted.

Additionally, after the saccades were detected using SacDet, they were excluded from further analyses based on their elevation component and saccadic latency. First, as the elevation component of the saccade should not be affected by the vestibulo-ocular nystagmus, saccades with an elevation component of more than 30 degrees off-target, were deemed 'guessing' and were excluded. Second, saccades that were made with a very short reaction time might have been anticipatory, while very long latencies might indicate that the participant did not see the stimulus, or was not paying attention. Thus, saccades with a latency shorter than 80ms and longer than 900ms were excluded. Finally, we excluded the dataset of subject S002, as due to technical difficulties, we could not complete the experiment.

2.7 Modelling

To quantify the accuracy of the subjects we first calculated the target location (T_R) on the retina of the subjects by correcting the target location in chair coordinates (T_c) for the position of the eye in space during stimulus onset (E_{on} , Eq. 1). Subsequently, we described shift in gaze ΔG as a result of the passive head movement due to the movement of the chair in space (ΔH_C), the active head movement in chair (ΔH_A) and eye-in-head movement (ΔE_H , Eq. 2).

$$T_R = T_c - E_{on} \quad (1)$$

$$\Delta G = T_R - a * \Delta H_C - b * \Delta H_A - c * \Delta E_H \quad (2)$$

To calculate the response gaze shift, we corrected the offset of the saccade in chair coordinates for the onset of the saccade in chair coordinates (Eq. 3).

$$\Delta G_{resp} = Sac_{off} - Sac_{on} \quad (3)$$

To see which of these variables would have to be incorporated to explain our results the best, we propose eight different models in total based on Eq.2, that each differ in compensating for either intervening passive head movements, active head movements or eye-in-head movements (Figure 1B, C). Figure 1A shows the temporal order of the chair-in-space, active head- and eye-in-head movements that are involved during these models.

As an example, Figure 1B shows the mechanisms of Models V and VIII (table 1). In Model V, the stimulus location is presented at T_0 , while the eye is located at $[0,0]$ and the initial location of the target is presented by T_R . However, due to intervening head- (ΔH_C and ΔH_A) and eye-movements (ΔE_H), the original location of the eye has shifted to a different location in space. Namely, at the location at the onset of the saccade (Sac_{on}). To produce a correct saccade from there, the visuomotor system should incorporate these movements. If this has been done properly, the right saccade will be made towards (T_0), as depicted by Model V. When the visuomotor system does not incorporate the head and eye-movements, a saccade equal to (T_R) will be made. However, the actual location of the eye is at (Sac_{on}), which results in a saccade that misses the target location. Figure 1C shows the mechanisms of all models, as depicted in table 1.

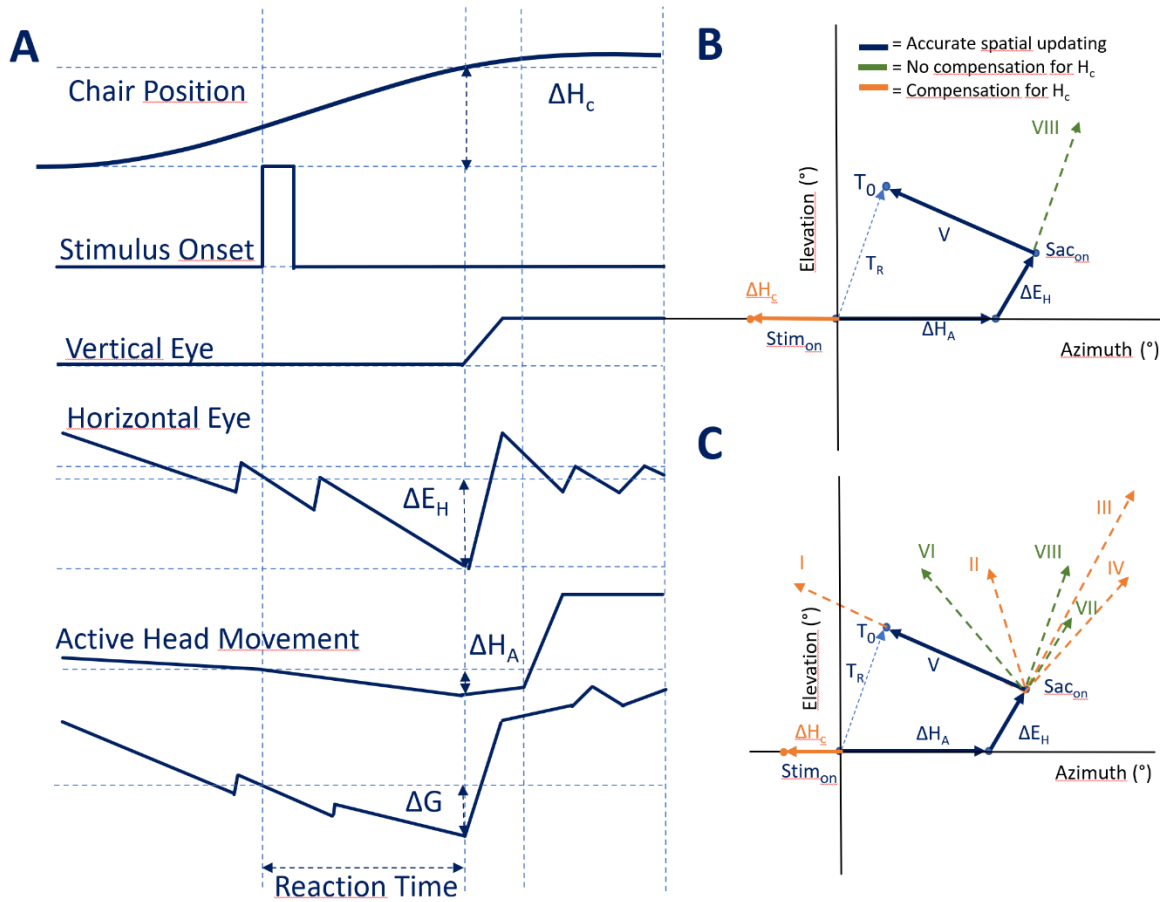


Figure 2: (A) The temporal order of the chair position, eye- and head-movements and cumulative shift in gaze. (B) Models V and VIII during passive body rotations, with active head movements and eye-in-head movements. (C) All models for spatial updating according to table 1. Models I to IV also compensate for head-in-chair movements (ΔH_c , orange). Models V to VIII do not compensate for head-in-chair-movements (green). Only Model V shows accurate spatial updating, as it incorporates ΔH_A and ΔE_H to produce a saccade towards T_0 .

Table 1: Theoretical coefficients of Eq. 1 for Models I to VIII.

Model	Description	a	b	c
With compensation for passive chair-in-space movement				
I (world-centred)	Full eye-head compensation	1	1	1
II	Head-only compensation	1	1	0
III (head-centred)	Eye-only compensation	1	0	1
IV	No compensation	1	0	0
Without compensation for passive chair-in-space movements				
V	Full eye-head compensation	0	1	1
VI	Head-only compensation	0	1	0
VII	Eye- only compensation	0	0	1
VIII (retinocentric)	No compensation	0	0	0

2.8 Statistics

To quantify the performance of the subjects during the localization of visual stimuli of different stimulus durations, for each model we performed a linear regression analysis with the desired gaze shift ΔG as independent variable and the gaze response ΔG_{resp} as dependent variable for each participant separately (Eq 4). For each linear regression model, the gain (β_1), which is the slope of the regression line and the bias (β_0), which represents the intercept of the model were determined.

$$\Delta G_{resp} = \beta_0 + \beta_1 * \Delta G \quad (4)$$

In this model, the gain indicates that for every degree of ΔG , we can expect ΔG_{resp} to increase by β_1 . In other words, if the gain is 1, the average localization was perfect (if the bias is not included). If the gain is lower than 1, there is an underestimation of the response. Vice versa, if the gain is higher than 1, there is an overestimation of the response in relation to the target location. The bias represents the systematic error that is present throughout all responses, in relation to the fitted values. A high bias is usually associated with incorrect calibration or a systematic deviation by the subject, independent of the target location.

To address the goodness-of-fit of our model, we determined the coefficient of determination of our fitted linear model (R^2). In general, the R^2 represents the percentage of the response variable variation that is explained by our linear model. Thus, we use the R^2 to determine how well our model for ΔG_{resp} fitted the data. In addition, we computed the root mean squared error (RMSE) of the regression model. The RMSE measures the mean error of our responses to the predicted values of the linear model. Whereas the R^2 is the relative measure of the fit, the RMSE represents the absolute measure of the fit and can be interpreted as the standard deviation of the unexplained variance.

Furthermore, to statistically verify whether there was a significant effect of the stimulus duration on the reaction times, probit curves of the reaction times versus the cumulative probability were determined per stimulus duration for each participant. Subsequently, nine data points between the 20th and 80th percentile of the probit curves for each stimulus duration were pooled over all participants. The 20th and 80th percentile were chosen, as the probit curves were linear between these points. Subsequently, these data points were used in a linear regression analysis with the cumulative probability as independent variables, the reaction times as dependent variables and the stimulus durations as categorical variables. As we centred our data, the intercept represented whether the average reaction times depend on the stimulus duration. Meanwhile, the gain represented the spread of the reaction times. Finally, we performed an ANOVA-test to evaluate the whether the differences in reaction times in relation to the stimulus reactions were significantly different from each other. To assess which of the stimulus durations' reaction times were significantly different we performed a post-hoc Tukey-test.

3. Results

3.1 Gaze saccade consists of an Eye and Head component

To illustrate an example of a single saccade during head-free localization, Figure 3A shows the contribution of the shift in eye- and head position to the total gaze shift over time. First, at $t=70\text{ms}$, the eye- (green) and the head response (orange) moved towards the target location. After the eye had reached the target location, the head movement followed, which caused the VOR to redirect the eyes towards the centre of the head. Cumulatively, the shift in eye- and head position made up the gaze response (purple) that fixated on the perceived target location. After a brief fixation on the target location, it seemed the eye (and by extension, the gaze) moved further to the right, as a result of the slow-phase of the vestibulo-ocular nystagmus.

This phenomenon is also observable in Figure 3B, which illustrates the response traces of the eye (green), head (orange) and gaze (purple) in space. After stimulus onset, the initial response of the eye was directed towards the perceived target location at $[-30 -20]$ deg. Subsequently, it seemed that the eye movement moved towards the right on the azimuth, before making a saccade back to the central SLC at $[0,0]$. However, both the elevation component of the gaze and eye, and the head movement do not seem to be affected by this drift. Which further underlines the presence of the slow-phase of the vestibulo ocular nystagmus, as a result of the rotation of the chair.

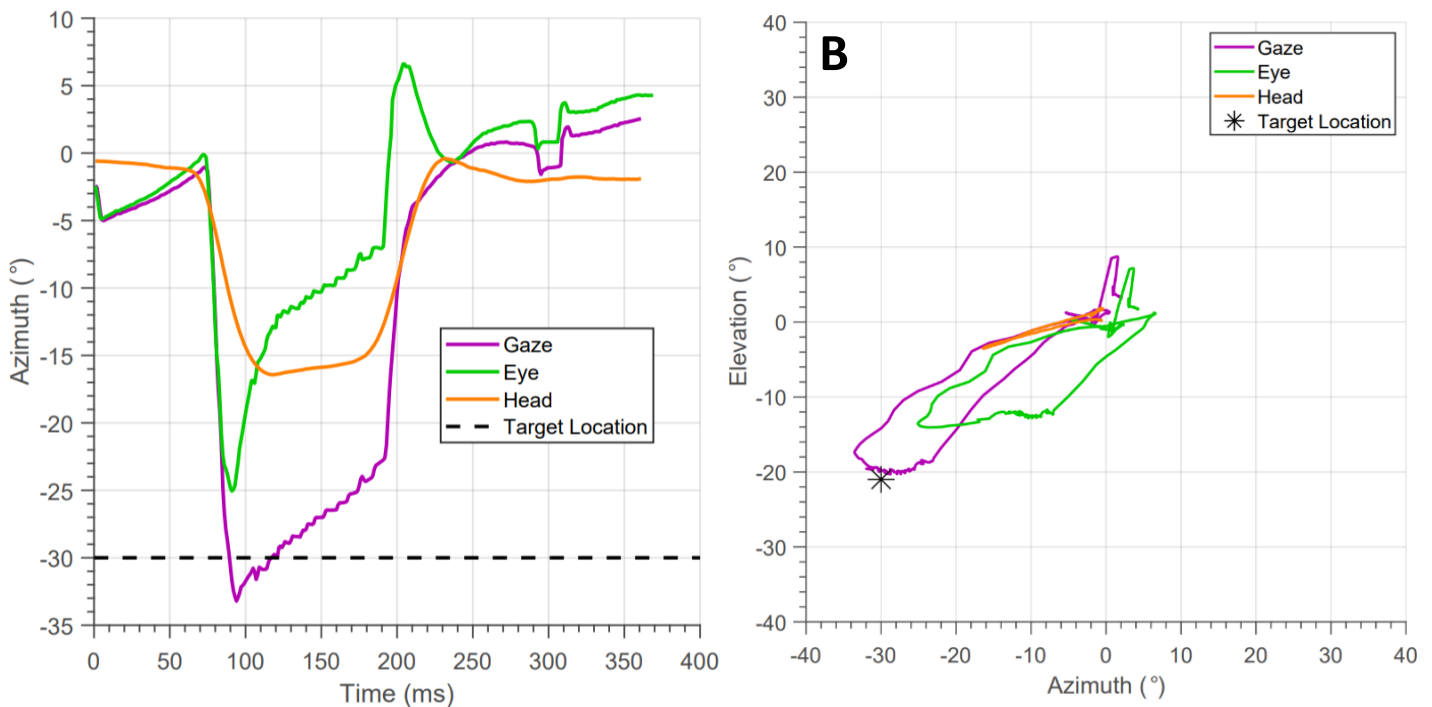


Figure 3: (A) illustrates an example of a single saccade for the gaze (purple), eye (green) and head (orange). The x-axis represents the time in ms, and the y-axis represent the azimuth in ($^{\circ}$). The black dotted line represents the azimuth coordinate of the target location. (B). The azimuth- (x-axis in ($^{\circ}$)) and elevation components (y-axis in ($^{\circ}$)) of the trajectories of the gaze, eye and head are shown. The black Asterix represents the target location.

3.2 Target vs. Response in chair coordinates

To investigate the localization behaviour for all trials per subject, we plotted the target locations versus response locations in coordinates related to the VC (T_C vs. Sa_{Coff}). In other words, there was no correction for the original retinal location, or intervening eye and head movements. In Figure 4, it is shown that there was an overshoot, which depended on the target location, in the localization performance of this subject (S003). This is indicated by the gains, which are higher than 1 for all stimulus durations. Moreover, there was a minor negative bias between -0.54° and -2.55° for all stimulus durations, which indicated a systematic underestimation of the target location, independent of the target location. However, there was an increasing trend to be observed of the R^2 in relation to the stimulus durations, whereas there was no trend to be observed in either the gain or the bias between stimulus durations. This demonstrates that, at least for this specific subject, the goodness-of-fit for each linear model was increased for longer stimulus durations.

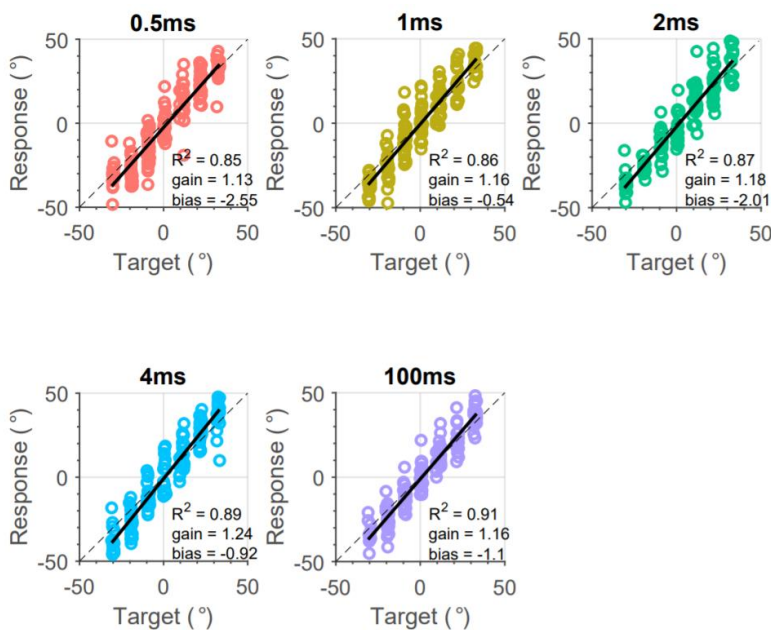


Figure 4: Target Response of subject S003 for the head free condition. The x-axis represents the target location in chair coordinates (T_C). The y-axis represents the offset of the saccade of chair coordinates. (b) is the gain and R^2 is the coefficient of determination of the regression. Stimulus durations [0.5 1 2 4 100]ms are shown.

When the results of the localization behaviour for all subjects are combined, the boxplots from figure 5 show that for the head free condition, there are large inter-individual differences between the subjects for the gain, R^2 and the bias. The exact values are provided by table 1 in the supplementary information. For the gain, the large whiskers in the boxplot originated from one subject (S004) that displayed a gain between 1.43 and 1.60 for all stimulus durations, while another subject (S005) had a gain between 0.59 and 0.70. However, when looking at the range of the boxes and the medians, the gain for all stimulus durations is above 1, which indicates an overshoot during target localization. However, similar to the trend in Figure 4, the goodness-of-fit of the linear models (R^2) increased as the stimulus durations got longer. For the bias, the range and medians are located just below 0, indicating a systematic underestimation in all responses. The large whiskers of the boxplot are explained by the performance of subjects S004 and S005. Whereas subject S004 presented a high gain, its bias was between -7° and -9° . This is in contrast with S005, which displayed a low gain, but a bias between 3.5° and 6° during its trials.

In contrast to the head free condition, the inter-individual differences in head fixed condition were lower for the gain and bias, but higher for the R^2 . Whereas S005 displayed a low gain between 0.65 and 0.75, the gain for all other participants were situated around 1. When looking at the goodness-of-fit for these models, the R^2 is increased for the 2ms, 4ms and 100ms stimulus durations, compared the 0.5ms and 1ms conditions, as indicated by the range of the boxes. Again, the large whiskers for R^2 can be attributed to subject S005, which had an R^2 of 0.67 and 0.64 for the 0.5ms and 1ms condition, respectively. The results for the bias in the head fixed condition were similar to the results of the head free condition, which indicated a small systematic underestimation for all responses. The lower whiskers can be attributed to subject S004, which displayed a bias between -7.4° and -8.6° . However, in contrast to the head free condition, subject S005 did not display high bias (between 0.3 and 2.2).

In conclusion, Figure 5 shows that there were large individual differences between the subjects in both the head free and head fixed condition. Most importantly, the range between the performances of the subjects was smaller for the gain in the head fixed condition compared to the head free condition. In contrast, the range of the R^2 was larger in the head free condition than in the head fixed condition. However, whether this difference was significant is not clear. Notably, there was no compensation for either the stimulus location on the subjects' retina (R_t), nor the displacements of the eye-in-head (ΔE_H), active head movements (ΔH_A) and passive head movements (ΔH_C). As such, we assumed that each subject looked straight ahead at the beginning of each saccade. As this may not have been the case, it might explain the inter-individual differences between subjects.

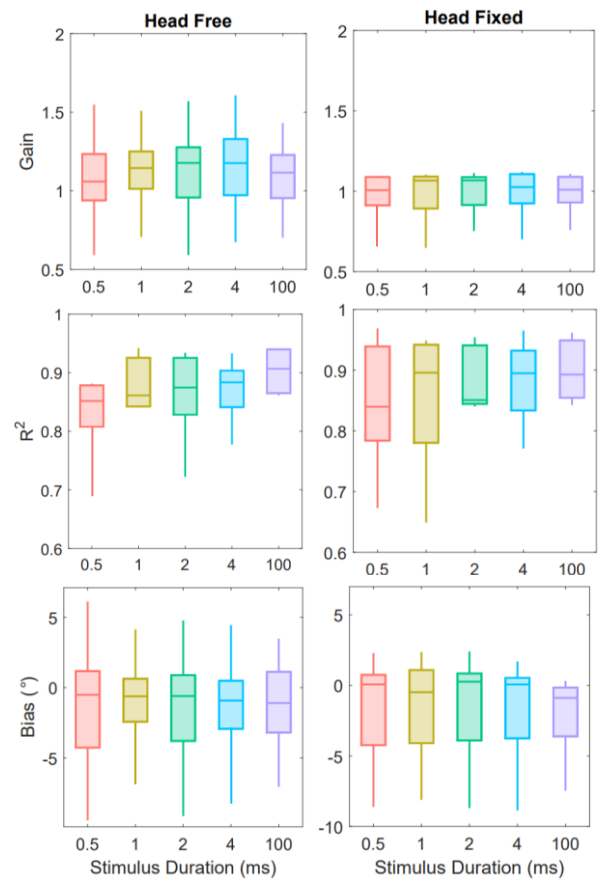


Figure 5: Boxplots for the gain (top), R^2 (middle) and bias (bottom) of the target response results of all subjects ($n=5$) during the head free- (left) and head fixed condition (right). The x-axis displays the stimulus duration that were presented to the subjects during the trials.

3.3 Target versus Response with different models.

To investigate whether the visuomotor system of our subjects compensated for intervening eye- and head movements, we analysed the data based our eight models. In Figure 6 the data are plotted for all models for one of the subjects.

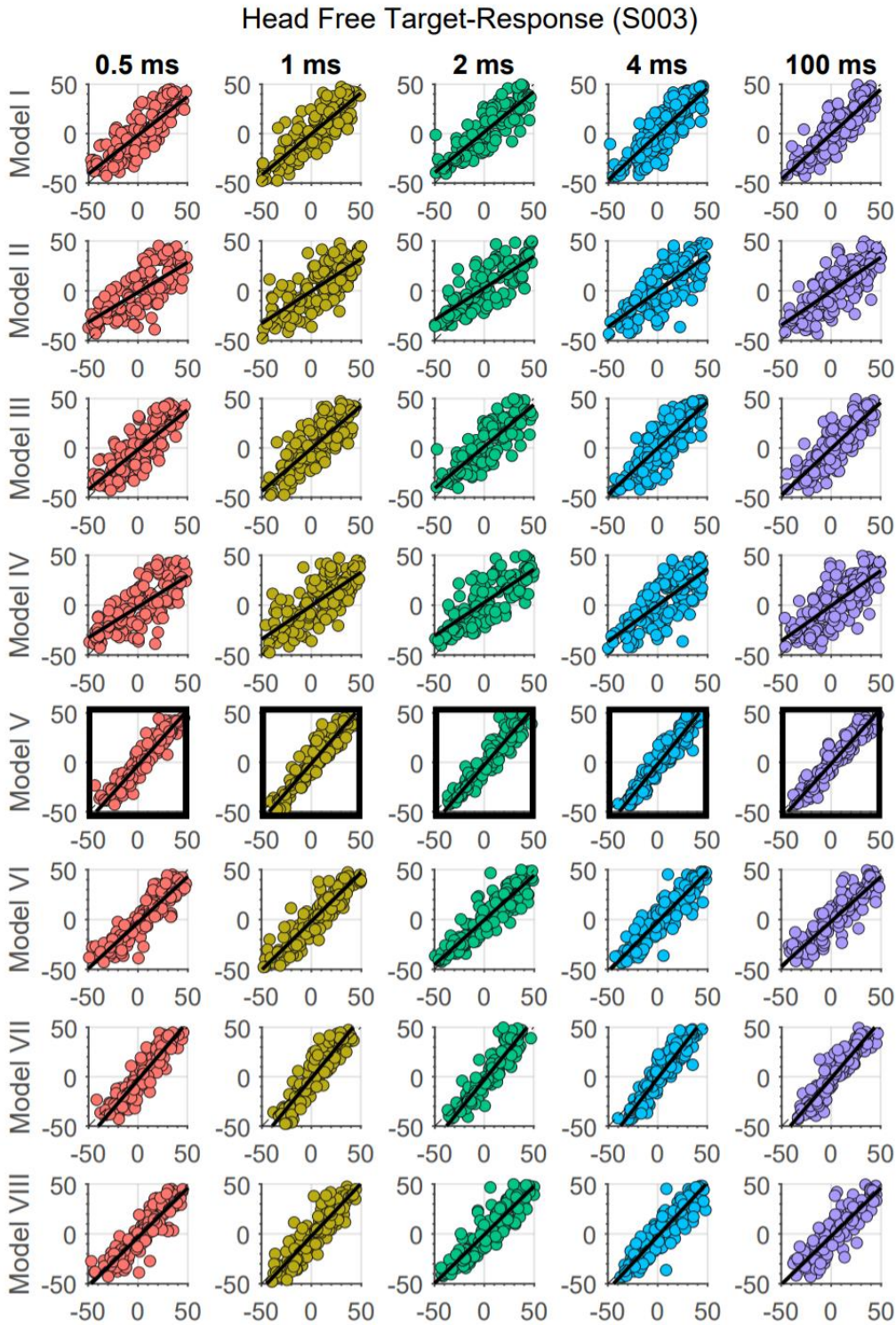


Figure 6: Head free target response for subject S003. The columns represent the various stimulus durations that were presented during the trials. The rows represent the various models that the visuomotor system can compensate for, according to table 1. On the y-axis are the azimuth coordinates for the response of the subject and on the x-axis are the azimuth coordinates of the adjusted target locations. In the graphs, the regression lines are plotted as black lines, whereas the black frames around the graphs represent the regression analysis with the highest R^2 for each stimulus duration.

Looking at Figure 6, the models that could best explain the performance of subject S003 based on the R^2 of the regression analysis, was model V. This model compensates for both the active head movement (ΔH_A) and eye-in-head movement (ΔE_H), but not for the passive head-in-chair movement (ΔH_C). As such, it is indicative of spatial updating. The R^2 , gain and bias for all models and stimulus durations are depicted in table 2. If we were to judge the models based on the gain, model VIII would explain the data from subject S003 the best, as it has gains which are very close to 1, especially for the 0.5ms condition. This would indicate that on average, the localization of this subjects was perfect and for all stimulus durations, and that the targets were localized from a retinocentric perspective. However, as the R^2 is much lower than the R^2 of model V, the fit of the regression model is worse than for model V. This also indicates that the spread of the responses around the regression line is higher for model VIII compared to model V. As such, we deemed that model V could best explain the performance of subject S003. When looking at the bias, one can observe that the 0.5ms condition has the lowest biases for all models. Strikingly, the models (I to IV) that compensated for the passive head movement (ΔH_C) displayed bias closer to zero than any of the models that did not compensate for passive head movements. This might indicate that there is a relation between the head movements and the bias in target localization. However, as we judged the success of our models based on the goodness-of-fit of the models (R^2), which were much lower for models I to IV, we excluded these models from further analysis. Nonetheless, the complete results are shown in the supplementary information (Supplementary tables 2-6).

Table 2: R^2 and gains of the performance of S003 for models I to VIII in the head free condition.

	0.5ms	1ms	2ms	4ms	100ms		0.5ms	1ms	2ms	4ms	100ms		0.5ms	1ms	2ms	4ms	100ms
Model	R^2						gain						bias				
I	0.66	0.72	0.75	0.74	0.77		0.78	0.83	0.82	0.92	0.91		-1.74	-0.32	1.56	-0.70	-0.63
II	0.56	0.62	0.68	0.63	0.62		0.60	0.65	0.64	0.72	0.68		-1.58	-0.39	2.67	-0.44	-0.53
III	0.63	0.68	0.71	0.68	0.71		0.80	0.86	0.84	0.93	0.94		-1.82	-0.60	1.50	-0.14	-0.71
IV	0.54	0.59	0.66	0.60	0.58		0.62	0.67	0.67	0.73	0.71		-1.66	-0.62	2.62	-0.10	-0.66
V	0.87	0.86	0.89	0.90	0.90		1.11	1.14	1.16	1.23	1.11		-3.01	-1.15	-2.77	-2.01	-1.43
VI	0.80	0.83	0.82	0.82	0.79		0.92	0.98	0.90	1.01	0.90		-3.14	-1.78	-0.46	-2.37	-1.94
VII	0.83	0.83	0.85	0.86	0.86		1.17	1.23	1.23	1.29	1.17		-3.19	-1.65	-3.15	-1.53	-1.66
VIII	0.79	0.82	0.82	0.81	0.77		0.99	1.06	0.98	1.08	0.97		-3.46	-2.37	-0.84	-2.27	-2.37

Head Fixed Target-Response (S003)

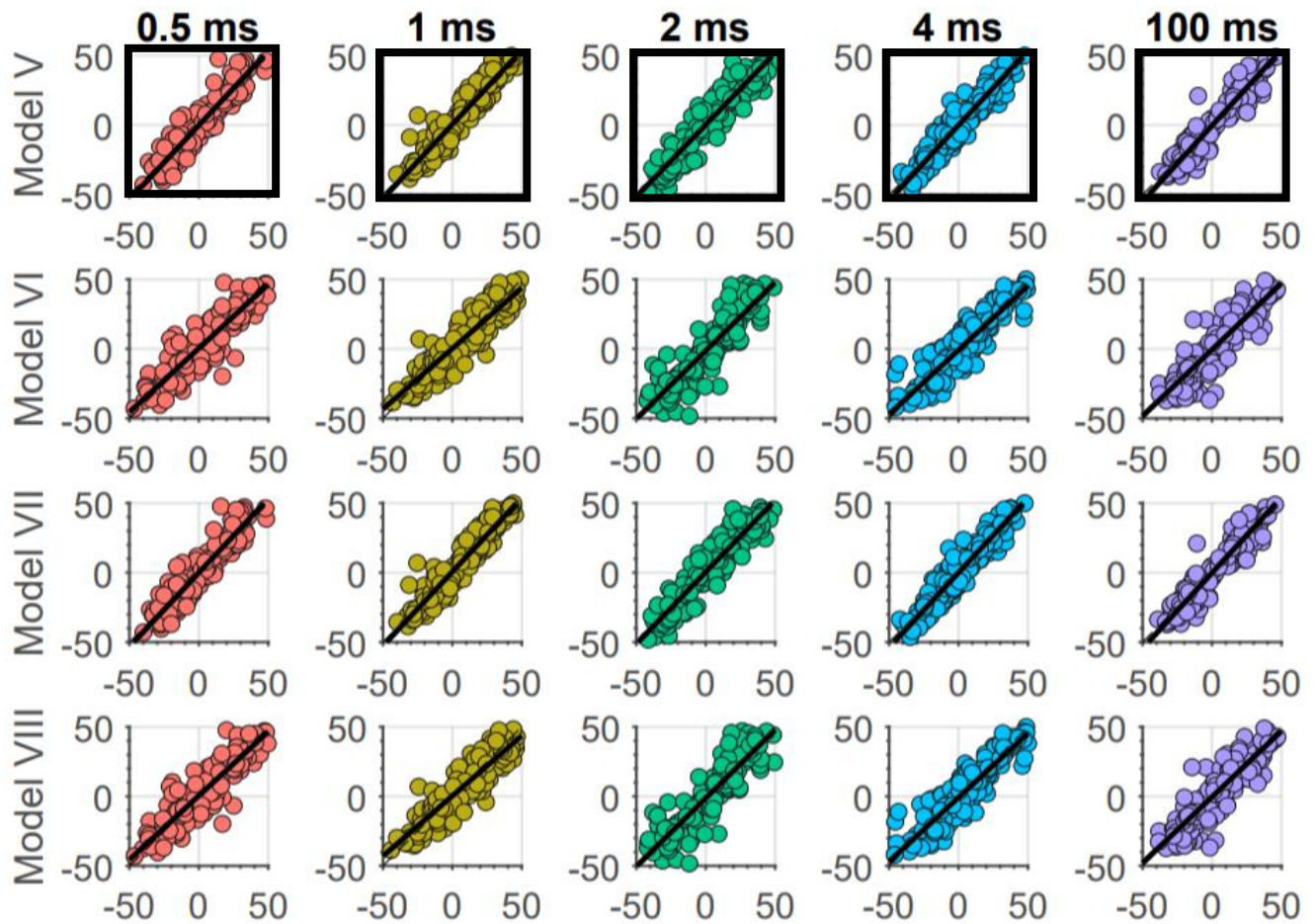


Figure 7: Head fixed target response for subject S003. The columns represent the various stimulus durations that were presented during the trials. The rows represent models V to VIII that the visuomotor system can compensate for, according to table 1. On the y-axis are the azimuth coordinates for the response of the subject and on the x-axis are the azimuth coordinates of the adjusted target locations. In the graphs, the regression lines are plotted as black lines, whereas the black frames around the graphs represent the highest R^2 for each stimulus duration.

Table 3: R^2 , gains and biases for models V to VIII that were used quantify the performance of S003 for the head fixed condition.

	0.5ms	1ms	2ms	4ms	100ms		0.5ms	1ms	2ms	4ms	100ms		0.5ms	1ms	2ms	4ms	100ms
Model	R^2						gain						bias				
V	0.84	0.90	0.87	0.91	0.87		1.07	1.07	1.04	1.08	1.09		-0.16	0.50	0.27	-0.10	-0.32
VI	0.78	0.74	0.80	0.84	0.77		0.92	0.87	0.98	0.93	0.96		0.40	0.24	-1.33	-0.84	-0.55
VII	0.84	0.89	0.87	0.90	0.86		1.07	1.07	1.04	1.08	1.09		0.00	0.60	0.44	0.01	-0.17
VIII	0.78	0.74	0.80	0.84	0.77		0.92	0.87	0.98	0.92	0.95		0.52	0.34	-1.19	-0.73	-0.40

Similar to the head free condition, model V could best explain the performance of S003 for all stimulus conditions, based on the R^2 . However, model VII could also explain the data very well. In fact, it differs only slightly in both the R^2 and the gain. As model VII does not compensate for active head movement (ΔH_A), this vector might have been close to zero during the head fixed trials, as we suspected. Furthermore, the gains of models VI and VIII are close to 1, but the difference in gain between these models and models V and VII is less than in the head free condition. Interestingly, the bias for these models was close to zero, whereas the bias for models I to IV were higher (not shown, supplementary information). This is opposite of what we observed in the head free condition and may suggest a relation between head movement and bias. In conclusion, these results imply that during the head fixed condition, subject S003 also used spatial updating to localize its target.

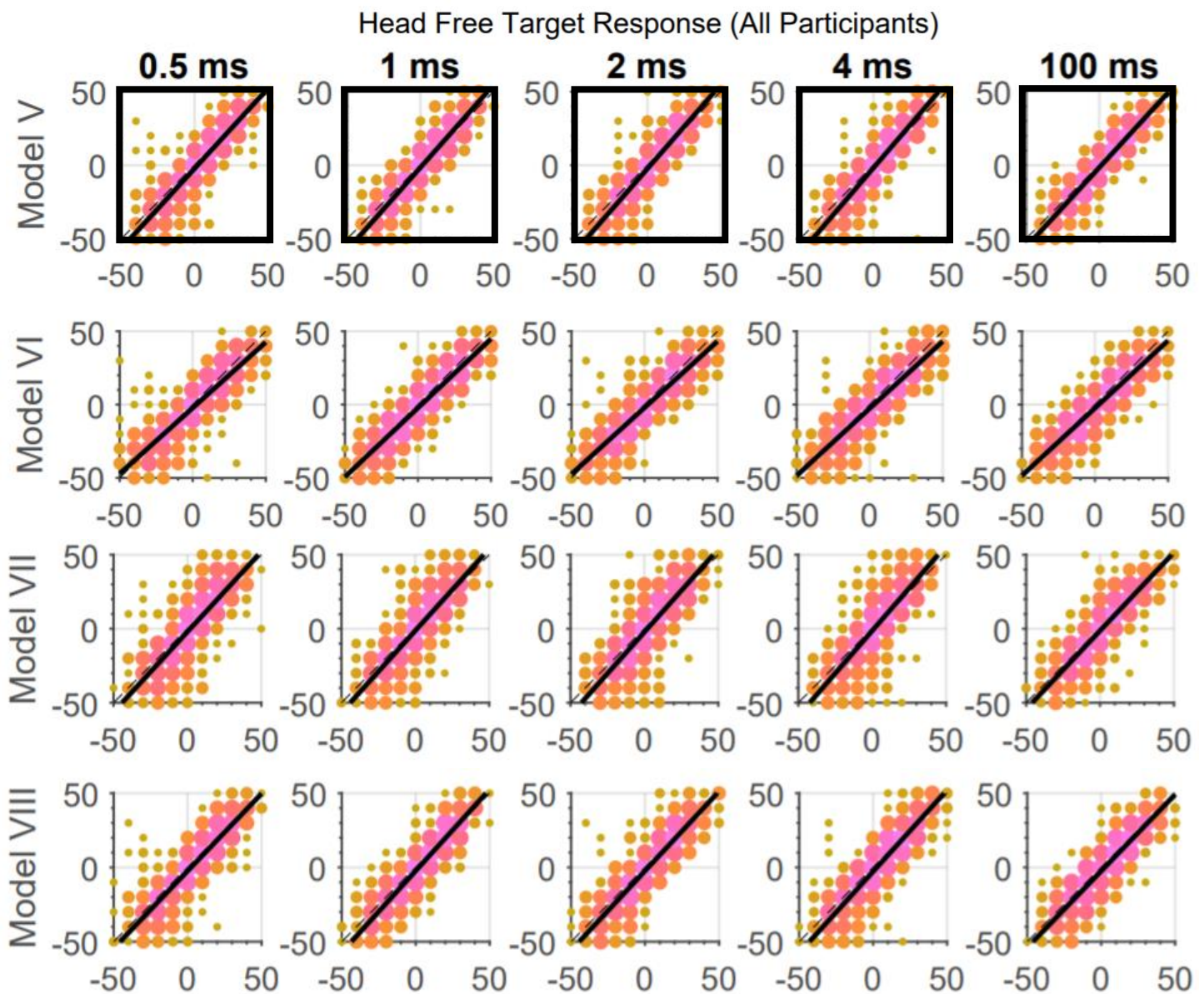


Figure 8: The stacked head free target response for all subjects. The columns represent the various stimulus durations that were presented during the trials. The rows represent the various models that the visuomotor system can compensate for, according to table 1. On the y-axis are the azimuth coordinates for the response of the subject and on the x-axis are the azimuth coordinates of the adjusted target locations. In the graphs, the regression lines are plotted as black lines, whereas the black frames around the graphs represent the highest R^2 for each stimulus duration.

When the performances of all participants were stacked for the head free condition, Model V still explained the results the best, based on the R^2 . Moreover, the gains for all stimulus conditions is closer to zero compared to the individual performance of S003. Nonetheless, the gains for all stimulus conditions are the closest to 1 for model VIII. However, the R^2 is still worse compared to Model V, indicating that the spread of the responses around the regression line is larger compared to Model V. It is important to note that the performances from Figure 8 are based on the individual responses of all subjects combined. As such, there is a danger that a high gain from one subject and a low gain from another subject, would ultimately result in a gain that is close to 1.

When looking at the individual performances for Model V to VIII for all stimulus conditions during the head free condition in Figure 9, one can observe similar inter-individual differences as in Figure 5. For the gain, there were large inter-individual differences between the subjects, as indicated by the range of the boxes and the large whiskers for Model V, VII and VIII. However, these differences did not seem to change between models. Furthermore, the medians of the gain were above 1 for Model V and VII, below 1 for Model IV and centre around 1 for Model VIII. The inter-individual differences for the bias were also present, but similar the Figure 5, the medians were just below 0 for all stimulus

duration. Finally, the shape of the boxes and whiskers of the R^2 were similar between the models. However, Model V had the highest median for R^2 in all stimulus duration.

In summary, the results from both the individual responses combined (Figure 8) and the individual performances separate (Figure 9) demonstrated that for the head free condition, our results could best be explained by Model V, indicating spatial updating. Whether the subjects displayed an overshoot or undershoot of the responses, varied between individuals and not between models. Finally, in all models, there seemed to be an overall systematic underestimation for all target response, independent of the target location.

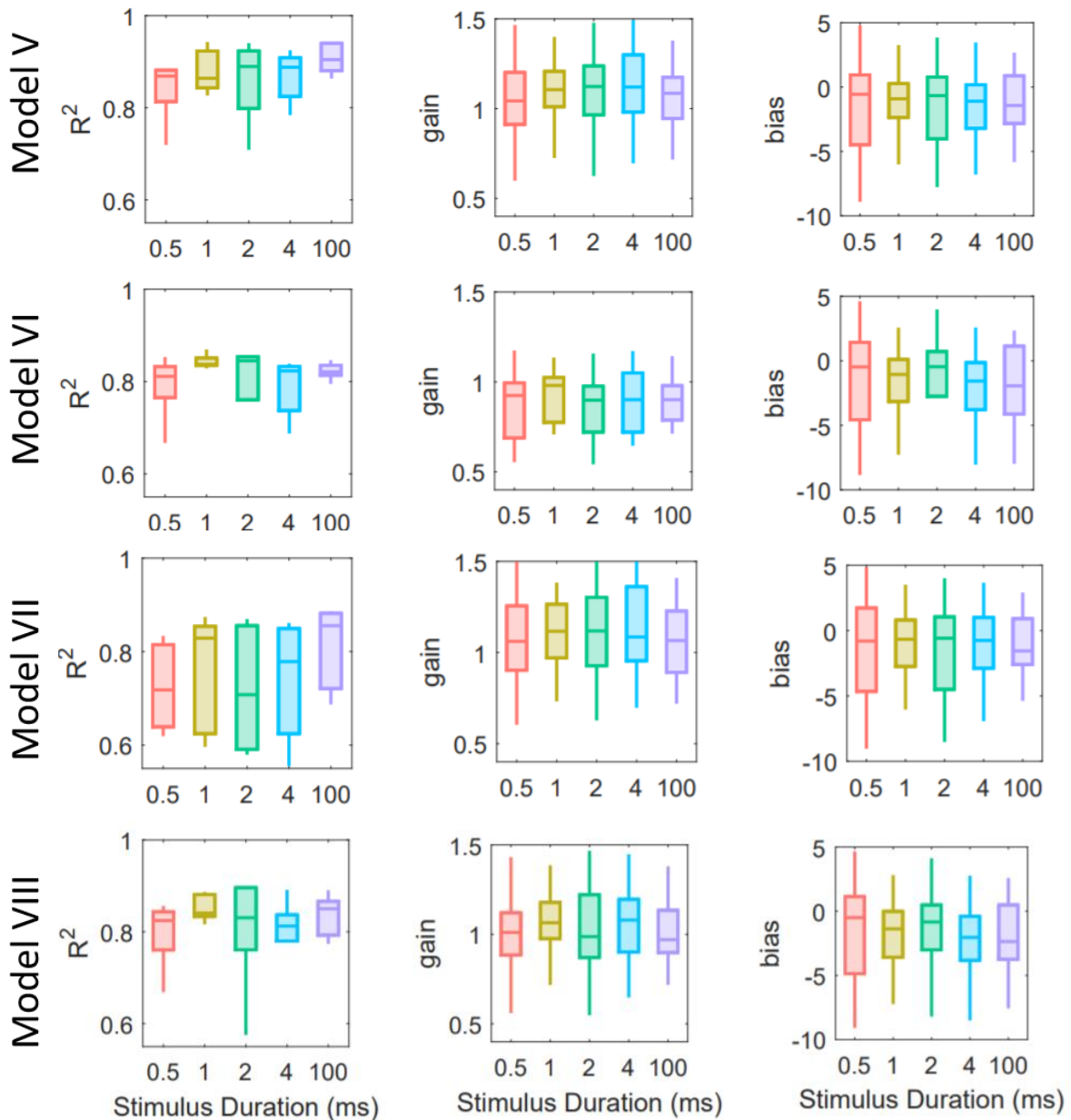


Figure 9: Boxplots of the individual performances for Models V to VII for all stimulus conditions during the head free condition. Each row represents the results of a model. The first column depicts the R^2 , the second depicts column the gain and the third column represents the bias in degrees. On the x-axis depicts the different stimulus condition.

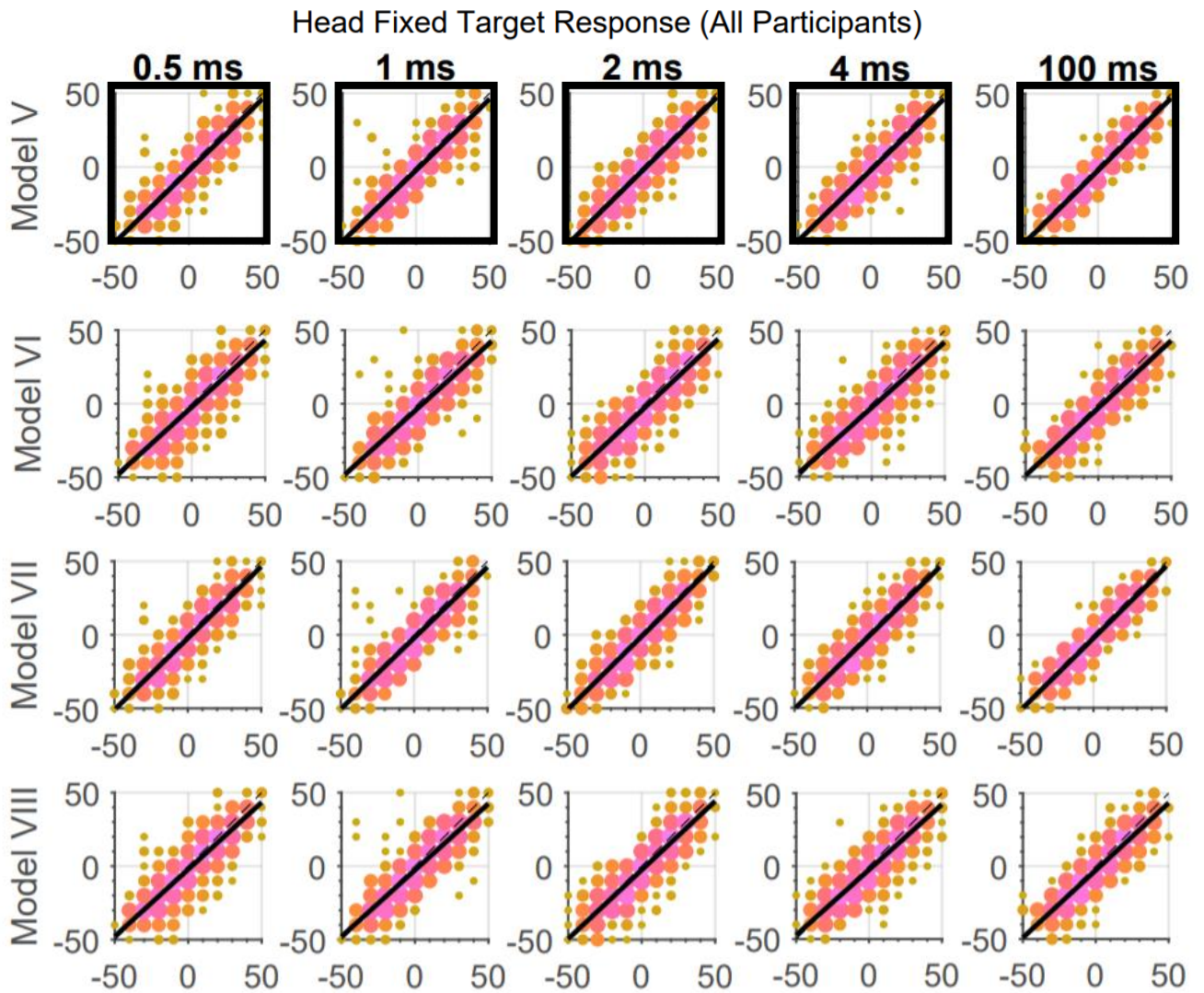


Figure 10: The stacked head fixed target response for all subjects. The columns represent the various stimulus durations that were presented during the trials. The rows represent the various models that the visuomotor system can compensate for, according to table 1. On the y-axis are the azimuth coordinates for the response of the subject and on the x-axis are the azimuth coordinates of the adjusted target locations. In the graphs, the regression lines are plotted as black lines, whereas the black frames around the graphs represent the highest R^2 for each stimulus duration.

Similar to Figure 8, Figure 10 shows that the model that best explained the localization behaviour of all responses combined, was model V. However, in contrast to the head free condition, these stacked performances of the head fixed condition show that model V displays both a high R^2 , as well as a high gain (exact values shown in supplementary figures). Again, compared to the individual performance of subject S003 in Figure 7, model VII is very similar to model V for the head fixed condition.

When looking at the individual performance for all subjects in Figure 11, the most notable difference is that the inter-individual differences are smaller compared to the head fixed condition. Moreover, the gains for Model V are located around 1. However, the inter-individual variety in performance is larger for the R^2 , compared to the head free condition. Nonetheless, one can still observe that for Model V and for Model VII, the R^2 is the highest throughout all models. Regarding the bias, there are large inter-individual differences, which do not differ between models. However, the majority of the boxes' range is below 0.

All in all, we conclude that for the head fixed condition, our subjects used spatial updating to localize the target location for all stimulus conditions, as indicated by the gains close to 1 and highest goodness-of-fit for Model V. Moreover, there seems to be a small systematic underestimation throughout all targets. Interestingly, Model VII performs very similar to Model V. As Model VII does not compensate for active head movement, this result is expected for the head fixed condition.

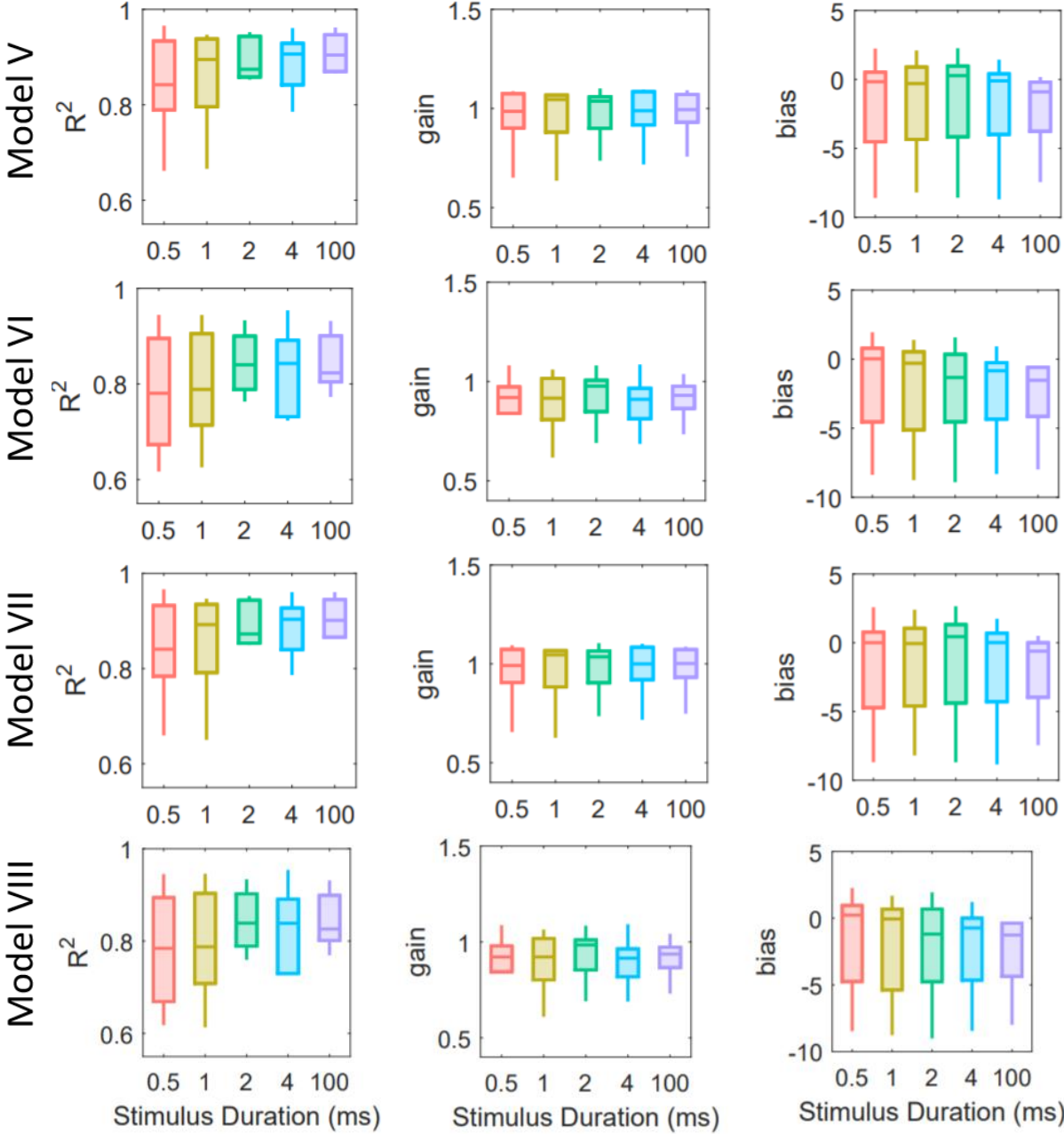


Figure 11: Boxplots of the individual performances for Models V to VII for all stimulus conditions during the head fixed condition. Each row represents the results of a model. The first column depicts the R², the second column the gain and the third column represents the bias in degrees. On the x-axis depicts the different stimulus condition.

3.4 Stimulus duration versus Reaction times

To determine whether or not the stimulus duration affected the reaction times of the subjects, the reaction times were plotted against the cumulative probability in a probit plot. As the probit plots for the head free condition looked similar to the probit plots of the head fixed condition, only the head fixed condition is shown in Figure 12. The probit plots for the head free condition are shown in the supplementary Figures.

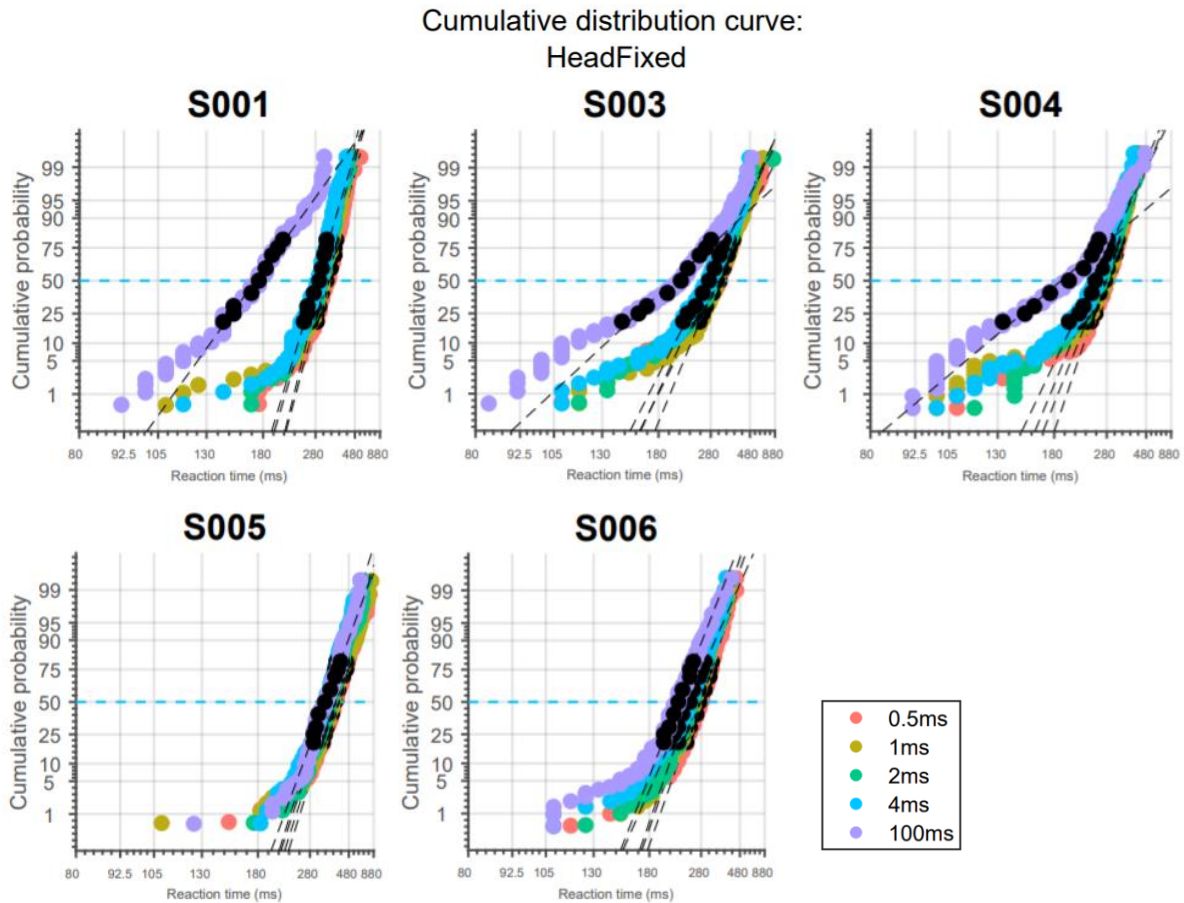


Figure 12: Probit plots of the cumulative distribution of the reaction times for the head fixed condition, for all participants. The y-axis displays the cumulative probability of the reaction times in (ms), which are displayed on the x-axis.

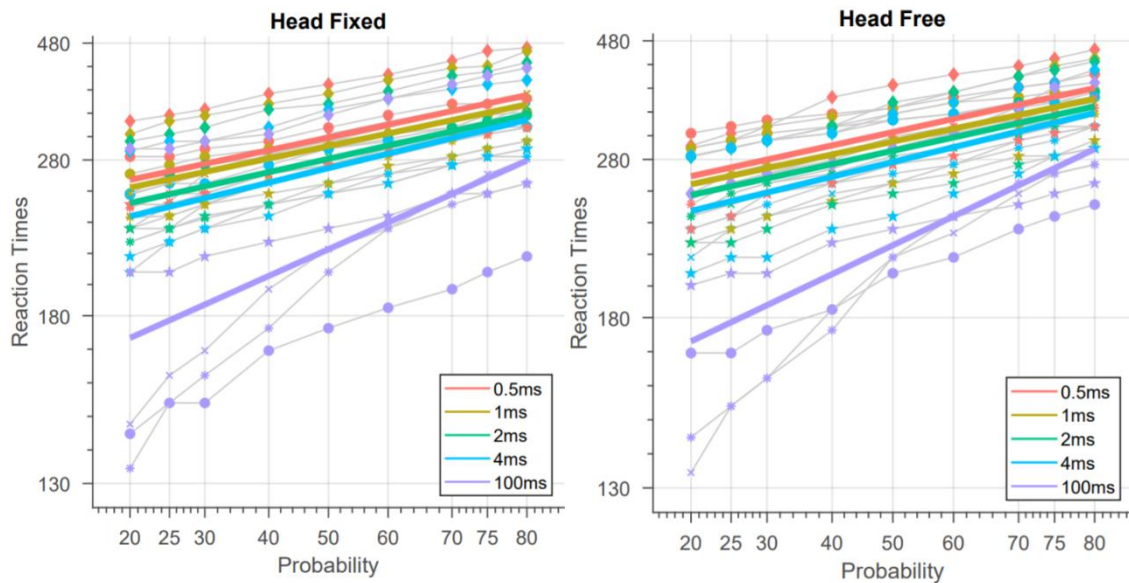


Figure 13: The probability (x-axis) versus the reaction times (y-axis) for the categorized stimulus durations. For each participant, we extracted 9 data points between the 20th and 80th percentile and categorized them by stimulus condition. The markers each represent a participant, whereas the coloured lines represent the regression lines of the linear models that was fitted through the data points of each category.

To determine whether or not there were significant differences between the reaction times of each stimulus duration, we categorized 9 datapoints from each participant between the 20th and 80th percentile based on their stimulus duration (Figure 13). Subsequently, we performed a multiple regression analysis to investigate whether or not the reaction times were dependent on the stimulus duration. Finally, we performed an ANOVA to determine if there was an overall significant difference between the stimulus durations and their reaction times.

For the head fixed condition, the ANOVA showed a significant main effect for the stimulus duration on the mean reaction times ($F(4,224) = 3.7558, p=0.006$). In other words, the mean reaction times for each stimulus duration, were significantly different from each other. Moreover, there was an overall significant effect for the slope of the regression lines on the stimulus duration ($F(5,244) = 33.68, p<0.001$), which indicates that the spread of the reaction times is dependent on the stimulus duration. Subsequently, the post-hoc Tukey test showed that the 100ms stimulus duration was significantly different from all other stimulus durations. As such, the significant results from the ANOVA-test could be entirely attributed to the interaction of the 100ms stimulus duration with the 0.5ms-, 1ms-, 2ms- and 4ms stimulus duration ($p<0.001$ for all interactions with 100ms). Between the 0.5ms-, 1ms-, 2ms- and 4ms stimulus durations, there were no significant differences.

During the head free conditions, similar results were obtained. The ANOVA-test showed that the mean reaction times were dependent on the stimulus durations ($F(4,224) = 6.38, p<0.001$) and that the spread of the reaction times were dependent on the stimulus durations as well ($F(5,224) = 79.26, p<0.001$). Moreover, the post-hoc Tukey test showed that these effects were due to a significant difference between the 100ms- and the other stimulus durations ($p<0.001$ for all). Between the other stimulus durations, there were no significant differences.

All in all, we conclude that for both the head fixed- and head free condition, the reaction times for the 100ms stimulus duration were significantly different compared to the 0.5ms-, 1ms-, 2ms- and 4ms stimulus durations. However, there were no differences between these stimulus durations.

4. Discussion

In this internship report, we aimed to further elucidate on the mechanisms of spatial updating during visual localization experiments with vestibular input, based on the study done by Van Barneveld et al.²³. During our experiments, the goal for the subjects was to localize visual flashes of different stimulus durations, that were fixed to the vestibular chair, which rotated sinusoidally. Furthermore, we asked the subjects to keep their head still, or to incorporate active head movements when attempting to localize the presented stimuli.

Our results show that for the head free condition, the performances of our subjects could best be described by model V, as indicated by the gain close to 1 and high goodness-of-fit for this model (R^2). In other words, when the visuomotor system compensated for the intervening active head movements and eye-in-head movements, but not for the passive head movements. This indicates that spatial updating was used. Moreover, there were large inter-individual differences between the subjects, which caused a widespread within the gain and bias. As such, whether a subject displayed an over- or undershoot, dependent on the subject itself. However, it did not affect our conclusion of which model could best explain the data, as the inter-individual differences were consistent across all models. Finally, despite the large inter-individual differences in the gain, the overall goodness-of-fit of the models did increase for longer stimulus duration, indicating that the overall localization performance increased with the stimulus duration.

During the head fixed condition, Model V could also explain our data best. However, there were some notable differences between the two conditions. First, the inter-individual differences within the R^2 were larger and the median was lower in the head fixed condition. However, the differences between the gains were smaller and the median was close to 1. In other words, the target localization of all subjects was more precise and accurate, but the goodness-of-fit for these models varied widely, especially for the shorter stimulus conditions (0.5ms and 1ms). Moreover, there was a slight systematic underestimation of the target location during this condition, as indicated by the bias lower than 0. Strikingly, Model VII performed nearly identical to model V when evaluating which model could best explain our data. Model VII only compensates for intervening eye-in-head movements and does not incorporate for active head movements (ΔH_A) and the task for our subjects during the head fixed condition was to keep their head still. As such, it is most likely that there was no active head movement to compensate for and that the subjects looked relatively straight ahead. During the head free condition, the subjects were allowed to move their head. This implies that if a subject failed to return their head towards the centre after a gaze response, the head may not be straight ahead for the subsequent trial. Thus, if the head movements were compensated for, we would expect Model VII to perform worse than Model V, and that is what the data showed. Finally, Model VIII also showed that the median of the gains was close to 1 for the head free conditions for all participants, but specifically for subject S003. This implies that subject S003 might have located the visual flash from a retinocentric perspective, without compensating for either intervening passive- or active head movement, or eye-in-head movements. However, the explained variance of this model (R^2) was lower than for Model V, which indicated that this model did not fit the data as well as Model V. Thus, we concluded that subject S003 did not locate the target from a retinocentric perspective, but rather used spatial updating and overestimated the target location.

The large inter-individual differences in the performance of our subjects might be related to the fact that four out of five subjects wore either glasses or lenses. As these subjects did not wear glasses during the experiments, the target may fall in front or behind the retina, for myopia and hyperopia,

respectively. This may cause a blurry image, which negatively affects visual target localization²⁸. Moreover, if a subject had astigmatism, the diffraction of light from the distorted cornea could create a retinal smear for stationary visual stimuli.

In Models I to IV, which compensated for the passive head movements (ΔH_C), the performance was worse compared to the models that did not compensate for this type of movement. This is what we expected, as the stimuli were being presented in coordinates that are relative to the chair. If one were to present stimuli in world coordinates (e.g. on the wall), we would expect that the visuomotor system would have compensated for the movement of the chair. This is in line with the results of Van Barneveld²³. They showed that the head-in-space movement was accounted for when long stimulus duration targets (100ms) were presented in world coordinates relative to the chair. However, this type of head movement was not accounted for when long duration stimuli were fixed to the chair and this is what our data shows as well.

However, the results from Van Barneveld also showed that for shorter stimulus duration (0.5- and 4ms in world fixed and 0.5ms in chair fixed) there was no spatial updating. In other words, their subjects localized these stimuli from a retinocentric perspective. Meanwhile, in our results, there was spatial updating for these stimulus durations. One explanation for this discrepancy in results could be that we used eye trackers which have a sampling rate of 120Hz. Whereas Van Barneveld used a variant of the scleral search coil technique called the Double Magnetic Induction technique that has a sampling rate up to 500Hz²⁹. As such, their temporal precision is higher. However, we looked at the position of the eye and head between stimulus onset and saccade onset. In this relatively short time period, we expect that the eye did not move too much for the 500Hz sampling rate to be a large advantage over our 120Hz to have affected the results.

An additional explanation, irrespective of the findings of Van Barneveld, could be that the frequency with which we rotated the vestibular chair was too high. As the vestibular system essentially measures acceleration⁹, our rotation frequency might have provided enough vestibular information for our subjects to distinguish between target motion and self-motion, which is required for spatial updating, even during the shortest stimulus durations. However, we opted to use the same rotation frequency as Van Barneveld, which did not see spatial updating in their short stimulus duration. Other variables that could have influenced the vestibular perception are age and the gain in VOR. First, we had a relative young group of subjects (age = 26.8 ± 1.40 yrs.) and it has been suggested that motion perception deteriorates as humans get older³⁰. As such, the vestibular systems of our subjects might have been able to provide enough information regarding self-motion, compared to the subjects of Van Barneveld. Second, the VOR-gain also becomes worse as subjects get older. This results in a vestibulo-ocular nystagmus that is not equal to the movement of the head under vestibular stimulation³¹. Unfortunately, as the mean age of the subject of Van Barneveld is not mentioned in the paper, we cannot rely on these assumptions to have influenced the results. However, we could calculate the VOR-gain of our subjects compare them to the subjects of Van Barneveld to see whether or not this could have explained to discrepancy between our findings. Thus, future calculations could provide clarity on this matter. Nonetheless, the fact that our subjects did compensate for active head and eye-movements during even the shortest stimulus duration, instead of resorting to a retinocentric perspective, remains interesting.

In addition to a shorter rotation frequency and a wider range of visual stimuli, future studies could also vary in the intensity of visual stimuli. By incorporating this factor, one could establish a model of how vestibular input, stimulus duration and stimulus intensity relate to each other for accurate localization of objects in space. We expect that if either of these factors are ambiguous, the localization behaviour will be worse^{32, 33}. Looking beyond that, one could even add auditory stimuli into this model. When all these factors are combined, one could create a model which aims to explain how we identify objects around us in the natural world. Besides the accuracy of the response for different stimulus duration, we also investigated the relation between the stimulus duration and reaction times of the subjects. Our results showed that the reaction times for the 100ms stimulus duration was significantly shorter than for the 0.5ms-, 1ms-, 2ms, and 4ms stimulus duration. This is in line with literature, and follows the reasoning that if a stimulus is ambiguous or hard to detect, it yields less information to work with, and requires longer processing from the brain to make a decision³²⁻³⁴.

The results of this report contribute to the fundamental understanding of how humans can localize and interact with objects around them. However, these understandings could also be translated to the clinic. Due to the advancements in technology regarding eye tracking in the recent years, eye tracking has become more accessible for both researchers and patients alike. Moreover, the deterioration of both eye movements, as well as the vestibular system play a role during many neurodegenerative diseases^{35, 36}. As such, one could implement our set up to address and quantify these issues in patient with such a disease (e.g. Multiple Sclerosis). Eye tracking has been used to quantify oculomotor performance in patients with Multiple Sclerosis³⁷⁻³⁹. However, in these studies, the heads of the subjects are fixed, while they localize targets on a monitor, without vestibular input. Thus, these studies are not able to provide the same versatility as our vestibular chair set up, which limits their scope in investigating natural eye-movement behaviour. Moreover, they do not implement the different models that we use to identify whether or not there is spatial updating. By using these models in the clinic, we might be able to gain more insight in the impairments of the visuomotor system in these patients.

In conclusion, the results of this internship report suggest that the visuomotor system of our patients used spatial updating to localize the targets if their heads were fixated to the chair. If our participants were free to move their heads, they also localized with spatial updating. Furthermore, it seemed that target locations were better localized as the stimulus duration increased. Finally, we also report a significant difference in the reaction times for the 100ms stimulus duration compared to the other stimulus durations, where the reaction times is significantly shorter for the 100ms stimulus duration.

References

1. Goossens HH, Van Opstal AJ. Local feedback signals are not distorted by prior eye movements: evidence from visually evoked double saccades. *Journal of neurophysiology* 1997;78:533-538.
2. Land M. Eye movements in man and other animals. *Vision research* 2019;162:1-7.
3. Klier EM, Angelaki DE. Spatial updating and the maintenance of visual constancy. *Neuroscience* 2008;156:801-818.
4. Panichi R, Botti FM, Ferraresi A, et al. Self-motion perception and vestibulo-ocular reflex during whole body yaw rotation in standing subjects: the role of head position and neck proprioception. *Human movement science* 2011;30:314-332.
5. Sommer MA, Wurtz RH. What the brain stem tells the frontal cortex. II. Role of the SC-MD-FF pathway in corollary discharge. *Journal of neurophysiology* 2004;91:1403-1423.
6. Cheng Z, Gu Y. Vestibular System and Self-Motion. 2018;12.
7. Crapse TB, Sommer MA. Corollary discharge across the animal kingdom. *Nature reviews Neuroscience* 2008;9:587-600.
8. Balslev D, Himmelbach M, Karnath H-O, Borchers S, Odoj B. Eye proprioception used for visual localization only if in conflict with the oculomotor plan. *J Neurosci* 2012;32:8569-8573.
9. Purves D. *Neuroscience* 2018.
10. Mauss AS, Vlasits A, Borst A, Feller M. Visual Circuits for Direction Selectivity. *Annu Rev Neurosci* 2017;40:211-230.
11. Reichardt WJJoCPA. Evaluation of optical motion information by movement detectors. 1987;161:533-547.
12. Zeki S. Area V5—a microcosm of the visual brain. 2015;9.
13. Britton Z, Arshad Q. Vestibular and Multi-Sensory Influences Upon Self-Motion Perception and the Consequences for Human Behavior. 2019;10.
14. Barmack NH. Central vestibular system: vestibular nuclei and posterior cerebellum. *Brain Research Bulletin* 2003;60:511-541.
15. Lowenstein O, Wersäll JJN. A functional interpretation of the electron-microscopic structure of the sensory hairs in the cristae of the elasmobranch *Raja clavata* in terms of directional sensitivity. 1959;184:1807-1808.
16. Goldberg JM, Smith CE, Fernandez C. Relation between discharge regularity and responses to externally applied galvanic currents in vestibular nerve afferents of the squirrel monkey. 1984;51:1236-1256.
17. Huterer M, Cullen KE. Vestibuloocular Reflex Dynamics During High-Frequency and High-Acceleration Rotations of the Head on Body in Rhesus Monkey. 2002;88:13-28.
18. Ranjbaran M, Galiana HL. Hybrid model of the context dependent vestibulo-ocular reflex: implications for vergence-version interactions. *Front Comput Neurosci* 2015;9:6-6.
19. Raphan T, Matsuo V, Cohen BJE. Velocity storage in the vestibulo-ocular reflex arc (VOR). 1979;35:229-248.
20. St George RJ, Day BL, Fitzpatrick RCJTJop. Adaptation of vestibular signals for self-motion perception. 2011;589:843-853.
21. Crawford JD, Vilis T. Axes of eye rotation and Listing's law during rotations of the head. *Journal of neurophysiology* 1991;65:407-423.
22. Merfeld DM, Park S, Gianna-Poulin C, Black FO, Wood S. Vestibular Perception and Action Employ Qualitatively Different Mechanisms. I. Frequency Response of VOR and Perceptual Responses During Translation and Tilt. 2005;94:186-198.
23. Van Barneveld DCPBM, Kiemeneij ACM, Van Opstal AJ. Absence of spatial updating when the visuomotor system is unsure about stimulus motion. *J Neurosci* 2011;31:10558-10568.

24. Vliegen J, Grootel TJV, Opstal AJV. Gaze Orienting in Dynamic Visual Double Steps. 2005;94:4300-4313.
25. Klein SA. Measuring, estimating, and understanding the psychometric function: a commentary. *Percept Psychophys* 2001;63:1421-1455.
26. Piéron HJLap. II. Recherches sur les lois de variation des temps de latence sensorielle en fonction des intensités excitatrices. 1913;20:17-96.
27. Ronsse R, White O, Lefèvre P. Computation of gaze orientation under unrestrained head movements. *Journal of neuroscience methods* 2007;159:158-169.
28. Hairston WD, Laurienti P, Mishra G, Burdette J, Wallace M. Multisensory enhancement of localization under conditions of induced myopia. *Experimental brain research Experimentelle Hirnforschung Expérimentation cérébrale* 2003;152:404-408.
29. Bremen P, Willigen RFVd, Opstal AJV. Applying Double Magnetic Induction to Measure Two-Dimensional Head-Unrestrained Gaze Shifts in Human Subjects. 2007;98:3759-3769.
30. Lich M, Bremmer F. Self-motion perception in the elderly. 2014;8.
31. Anson ER, Bigelow RT, Carey JP, et al. VOR Gain Is Related to Compensatory Saccades in Healthy Older Adults. 2016;8.
32. van Maanen L, Grasman RPPP, Forstmann BU, Wagenmakers E-J. Piéron's Law and Optimal Behavior in Perceptual Decision-Making. *Front Neurosci* 2012;5:143-143.
33. Kurylo DD, Chung C, Yeturo S, Lanza J, Gorskaya A, Bukhari F. Effects of contrast, spatial frequency, and stimulus duration on reaction time in rats. *Vision research* 2015;106:20-26.
34. Efron R. Effect of stimulus duration on perceptual onset and offset latencies. *Perception & Psychophysics* 1970;8:231-234.
35. Kattah JC, Zee DS. Eye movements in demyelinating, autoimmune and metabolic disorders. *Current opinion in neurology* 2020;33:111-116.
36. Serra A, Chisari CG, Matta M. Eye Movement Abnormalities in Multiple Sclerosis: Pathogenesis, Modeling, and Treatment. *Front Neurol* 2018;9:31-31.
37. Nij Bijvank JA, van Rijn LJ, Balk LJ, Tan HS, Uitdehaag BMJ, Petzold A. Diagnosing and quantifying a common deficit in multiple sclerosis. *Internuclear ophthalmoplegia* 2019;92:e2299-e2308.
38. Polet K, Hesse S, Cohen M, et al. Video-oculography in multiple sclerosis: Links between oculomotor disorders and brain magnetic resonance imaging (MRI). *Multiple sclerosis and related disorders* 2020;40:101969.
39. Grillini A, Renken R, Vrijling A, Heutink J, Cornelissen F. Eye movement evaluation in Multiple Sclerosis and Parkinson's Disease using a Standardized Oculomotor and Neuro-ophthalmic Disorder Assessment (SONDA)2020.